Functionalized $(X\text{-}PEO)_2\text{-}(PS\text{-}Y)_2$ Star Block Copolymers at the Interfaces: Role of Terminal Groups in Surface Behavior and Morphology

R. Gunawidjaja, S. Peleshanko, and V. V. Tsukruk*

Department of Materials Science and Engineering, Iowa State University, Ames, Iowa 50011

Received March 4, 2005; Revised Manuscript Received July 24, 2005

ABSTRACT: We focus on the role of functional terminal group combinations for $(X\text{-}PEO)_2\text{-}(PS\text{-}Y)_2$ heteroarm star copolymers with respect to their interfacial behavior and surface morphology. We synthesized a series of star copolymers with combinations of bromine, amine, TBDPS, hydroxyl, and carboxylic terminal groups. The study concluded that hydrophilic functional groups attached to hydrophobic chains and hydrophobic functional groups attached to hydrophilic chains resulted in the stabilization of the spherical domain morphology, rather than cylindrical morphology predicted for the given chemical composition of star copolymers. The replacement of functional groups of hydrophobic polymer chains was found to be even more effective in creating stable and very fine circular domain morphology. In addition, for $(COOH\text{-}PEO)_2\text{-}(PS\text{-}NH_2)_2$ star polymer the ionization of carboxylic terminal groups at higher pH led to greater solubility of PEO chains in the water subphase, which along with deionization of amine terminal group prevented the lateral aggregation of PS domains, further promoting the formation of nanoscale circular morphology.

Introduction

Novel macromolecular architectures such as highly branched and star-shaped block copolymers have been found to exhibit novel aggregation behavior[1−5] and complex intramolecular interactions[6] in solution, surfaces, and interfaces.[7−14] Unique morphologies were found in branched and star block copolymers that were not observed for linear block copolymers.[15−20] At the air−water interface, the behavior of star-shaped copolymer is qualitatively identical to linear systems; the hydrophobic chain collapses into globules while the hydrophilic chain spreads out to form pancake structure.[21,22] At high surface pressure, nonetheless, recent studies showed that crowding of hydrophobic PS chains at a single junction point in asymmetric heteroarm PEO-*b*-PS_m star polymer increased circular micellar stability.[23,24]

Recent studies have extended toward more sophisticated copolymer architectures ranging from H-shaped to π-shaped,[25,26] Vergina-star,[27] dumbbell-shaped,[28] ABC star-shaped,[29] and dendrimer-like star block copolymer[30] motivated and made possible by recent rapid development in controlled living polymerization (CLP) techniques.[31] Auxiliary to being amphiphilic, these copolymers can contain multiple junction points and degree of branching, can be symmetrical or asymmetrical, and can contain multiple types of functional terminal groups. To obtain polymers with such architectural intricacy, combining two or more polymerization techniques is required. This approach often leads to polymers with dissimilar end-functional groups whose influence is often overlooked in the subsequent study.

A number of studies have shown that end-functionalized homopolymers and block copolymers composed of a combination of hydrophobic and hydrophilic terminal groups have self-assembling ability.[32,33] Hydrophobic alkane (C_{12} and C_{16}) terminal groups attached to hydrophilic chains act as a constraint confining the end(s) at the surface, hence reducing the solubility in water.[34] The effect of the nature of terminal groups (hydrophobic or hydrophilic) on the aggregation of PEO homopolymers in solution has also been studied by small-angle neutron scattering (SANS). It was found to be significant even if it occupies only a small volume fraction (<0.1%). For instance, hydrophobic methoxy ($-O-CH_3$) terminal groups affected the clustering of PEO, and the opposite was observed for hydrophilic hydroxyl ($-OH$) functionalized PEO chains.[35] Compared to junction point functionalization, terminal functionalization was found to result in larger aggregates due to the stronger excluded-volume effect.[36] Different peripheral functional groups—proton (H), methyl (CH_3), *tert*-butyldimethylsilane (TBDMS), and hydroxyl (OH)—attached to 4,6-bis(6-(2,2′-bipyridyl))pyrimidine resulted in notable changes in the mean molecular area (MMA) (also known as surface area per molecule) at the air−water interface. For example, functionalization with bulky TBDMS groups showed the largest MMA, i.e., about 3.5 nm^2 vs only about 1.5 nm^2 for proton functionalized 4,6-bis(6-(2,2′-bipyridyl))pyrimidine.[33] Theoretical calculation for PEO chain conformation in aqueous solution showed that the effect of the terminal groups remains noticeable for molecular chains up to 250−500 monomer units long (molecular weight ca. 10 000−20 000).[37]

The surface behavior of amphiphilic copolymers at the air−water interface had been explored largely for various chemical architectures, such as AB, A_nB_n, A_nB_m, and $(AB)_n$ as a function of chain lengths and compositions,[38−42] surface pressure,[43] temperature,[39] film thickness,[44] and nature of the terminal groups.[45] These structures are commonly visualized with atomic force microscopy (AFM) or transmission electron microscopy (TEM). Depending upon whether the hydrophilic or the hydrophobic segment is dominant, a range of surface microstructures are usually observed for these amphiphilic

* To whom all correspondence should be addressed: e-mail vladimir@iastate.edu.

10.1021/ma050463v CCC: $30.25
Published on Web 09/15/2005

Scheme 1. Synthesis of (Br-PS)$_2$-(PEO-TBDPS)$_2$

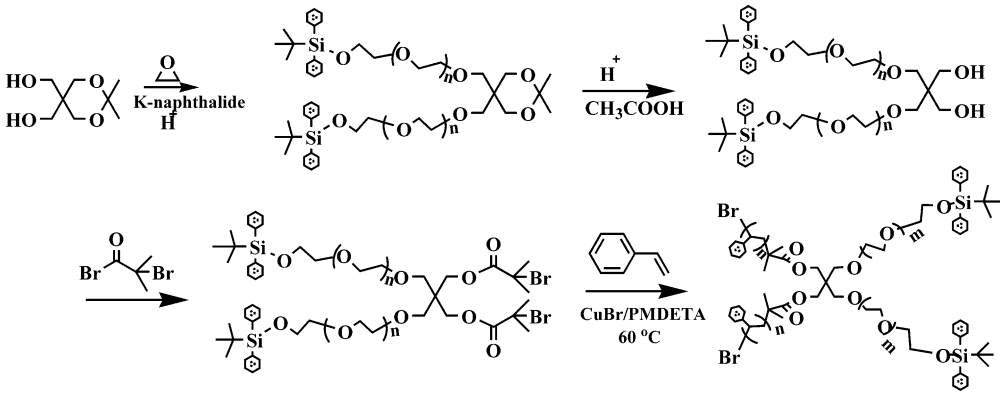

Table 1. Properties of Heteroarm Star Block Copolymers[a]

					NMR data					
		GPC data			PEO arm			PS arm		
no.	polymer	M_n, 10^3	M_w, 10^3	PDI	M_n, 10^3	N	ϕ	M_n, 10^3	N	total M_n, 10^3
1	(Br-PS)$_2$-(PEO-TBDPS)$_2$	14	18	1.31	7.5	170	0.32	14	135	43
2	(Br-PS)$_2$-(PEO-OH)$_2$	17	20	1.20	7.5	170	0.32	14	135	43
3	(Br-PS)$_2$-(PEO-COOH)$_2$	17	20	1.18	7.5	170	0.32	14	135	43
4	(NH$_2$-PS)$_2$-(PEO-TBDPS)$_2$	19	23	1.22	7.5	170	0.32	14	135	43
5	(NH$_2$-PS)$_2$-(PEO-OH)$_2$	17	21	1.22	7.5	170	0.32	14	135	43
6	(NH$_2$-PS)$_2$-(PEO-COOH)$_2$	16	19	1.20	7.5	170	0.32	14	135	43

[a] M_n is number-average molecular weight, M_w is weight-average molecular weight, N is number of monomeric units, and φ is volume fraction of PEO block.

copolymer systems. This includes ordered circular domains, randomly oriented spaghetti-like or lamellar morphology, mixed morphologies, and planar surface structures. By changing the nature of the terminal groups in amphiphilic block copolymer (PS-*b*-PVP/RX) with R = C_1 to C_{15} and X = I and Br, Zhu et al. demonstrated that the surface morphology of diblock copolymer is determined by the solubility of the hydrophilic chains.[45] A comprehensive study had been undertaken by Fauré et al. on the structure and phase transitions of PS−PEO diblock copolymer monolayers at the air−water interface for variable PEO chain lengths.[46]

It can be concluded that the changes in surface microstructure obtained through variation in chemical architecture, chain length, composition, surface pressure, temperature, and terminal group are merely the different ways of changing the arrangement of the hydrophilic chains at the interfaces. If the hydrophilic chains are not easily submersible in water phase, circular domains are formed. Decreasing dominance of hydrophilic chains leads to lamellar, mixed, and eventually planar microstructures. However, the role of the hydrophobic chain arrangement in determining the surface microstructure is not clearly understood. To date, surface studies on amphiphilic copolymers with variable terminal groups have mainly been limited to linear systems, and no studies had yet been reported on the effect of the terminal groups attached to different arms of amphiphilic heteroarm star copolymers.

In this work, we investigate the role of different terminal groups for both the hydrophilic and hydrophobic arms of A_2B_2 heteroarm star copolymer. We focus on four-arm star copolymer (X-PEO)$_2$-(PS-Y)$_2$ introduced in our recent studies.[23,24] We report chemical modification of these star copolymers and discuss their surface behavior at the air−water interface and the surface microstructure on a solid surface.

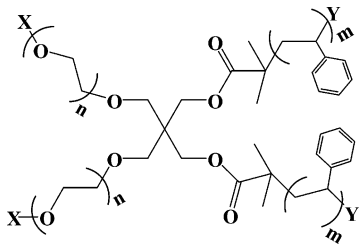

Figure 1. Chemical structure of 4-arm (X-PEO)$_2$-(PS-Y)$_2$ heteroarm star copolymers.

Experimental Section

Materials. Using 2,2-dimethyl-5,5-bis(hydroxylmethyl)-1,3-dioxane as a core, amphiphilic heteroarm PEO_2-PS_2 star copolymers were initially synthesized by growing two PEO arms by anionic polymerization of ethylene oxide, which was then terminated with a *tert*-butyldiphenylsilane (TBDPS) protecting group. Two polystyrene arms were then grown by atom transfer radical polymerization (ATRP) to make star copolymer (TBDPS-PEO)$_2$-(PS-Br)$_2$ (**1**), shown in Scheme 1. The detailed synthetic procedure for PEO_n-PS_m heteroarm star copolymers used here is described earlier.[47] These star-block copolymers possess a low polydispersity index, as confirmed by gel-permeation chromatography (GPC) and nuclear magnetic resonance (NMR) (Table 1). (In the molecular weight calculation using proton NMR, the TBDPS group was used as the reference peak. Without the TBDPS reference peak, molecular weights of the rest of the star copolymers are assumed to be the identical.) Hydrodynamic behavior of star copolymers in GPC measurement is responsible for the substantial difference in the measured molecular weight values with respect to those measured by NMR.[48] Chemical modification of polymer **1** yields a range of the 4-arm amphiphilic star copolymers (X-PEO)$_2$-(PS-Y)$_2$ with different terminal groups, X and Y (Figure 1). Table 2 shows the different combinations of terminal groups employed in this study. Here, "+" and "−" notations are used to assign the hydrophilic and hydrophobic groups or chains, respectively. To simplify the notation, we use a shorter abbreviation (X)$_2$-**S**-(Y)$_2$ with **S** standing for the star core and X and Y standing for different types of terminal groups (two groups for each type of arms).

Table 2. List of Functionalized (X-PEO)$_2$-(PS-Y)$_2$ Heteroarm Star Copolymers[a]

no.	polymer	abbreviations	notation[a]
1	(Br-PS)$_2$-(PEO-TBDPS)$_2$	(Br)$_2$-**S**-(TBDPS)$_2$	− − + −
2	(Br-PS)$_2$-(PEO-OH)$_2$	(Br)$_2$-**S**-(OH)$_2$	− − + +
3	(Br-PS)$_2$-(PEO-COOH)$_2$	(Br)$_2$-**S**-(COOH)$_2$	− − + +
4	(NH$_2$-PS)$_2$-(PEO-TBDPS)$_2$	(NH$_2$)$_2$-**S**-(TBDPS)$_2$	+ − + −
5	(NH$_2$-PS)$_2$-(PEO-OH)$_2$	(NH$_2$)$_2$-**S**-(OH)$_2$	+ − + +
6	(NH$_2$-PS)$_2$-(PEO-COOH)$_2$	(NH$_2$)$_2$-**S**-(COOH)$_2$	+ − + +

[a] Plus (+) is hydrophilic and minus (−) is hydrophobic.

The discussion in organized in the following manner: the hydrophobic PS chains of polymers **1**, **2**, and **3** are functionalized with hydrophobic Br functional groups, while the hydrophilic PEO chains are functionalized with hydrophobic TBDPS, hydrophilic OH, and hydrophilic pH-sensitive COOH functional groups. On the other hand, the hydrophobic chains of polymers **3**, **4**, and **5** are functionalized with hydrophilic, pH-sensitive amine functional groups, and the hydrophilic PEO chains are functionalized again with hydrophobic TBDPS, hydrophilic OH, and pH-sensitive hydrophilic COOH functional groups (Table 2).

Chemical Modification of Terminal Groups. Scheme 2 summarizes the synthetic procedures as described in the literature and presented briefly here. The treatment of polymer **1** (0.0154 mmol, 630 mg) with 1 M tetrabutylammonium fluoride, TBAF (1.54 mmol, 401.8 mg), in THF (25 mL) overnight gives polymer **2**.[49] ^{1}H NMR spectra demonstrate successful removal of TBDPS protecting group as indicated by the disappearance of peaks **a** and **b** in Figure 2a.

Polymer **2** (0.00266 mmol, 209 mg) was reacted overnight with succinic anhydride (0.053 mmol, 5.3 mg) in the presence of 4-(dimethylamino)pyridine, DMAP (0.00260 mmol, 0.32 mg), in pyridine (1.5 mL) to give polymer **3**.[50,51] The CH_2 signal of succinic acid is notated by letter **i** in Figure 2b. The ^{1}H NMR spectrum of (Br)$_2$-**S**-(TBDPS)$_2$ and ^{1}H NMR spectrum of (Br)$_2$-**S**-(COOH)$_2$ (δ, ppm, $CDCl_3$): 7.3−6.3 (m, 20H, aromatic),

Scheme 2. Synthetic Path for Functional Group Modification of (Br-PS)$_2$-(PEO-TBDPS)$_2$ and Conditions: (a) TBAF/THF; (b) Azidation by NaN_3/DMF; (c) P(Ph)$_3$/THF; (d) Hydrolysis by H_2O/THF; (e) Succinic Anhydride, DMAP/Pyridine

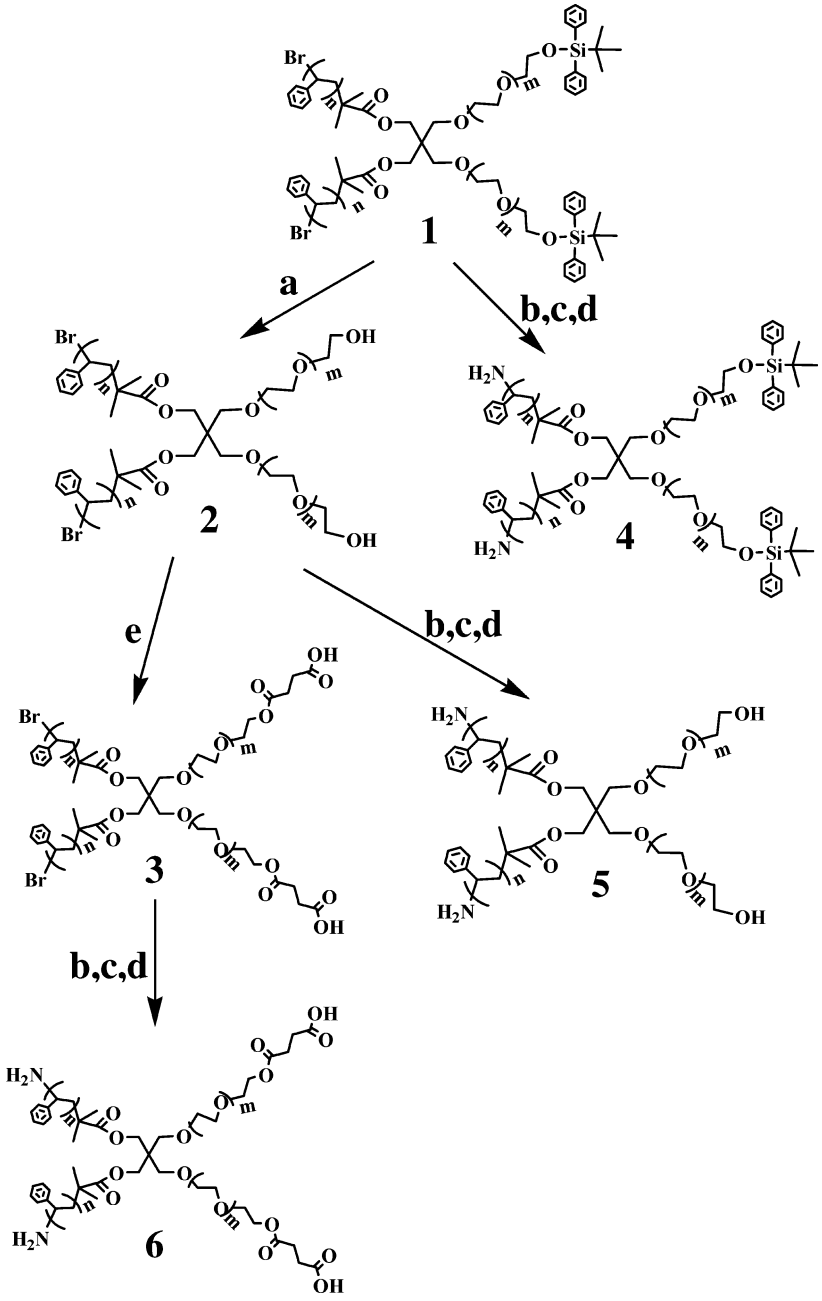

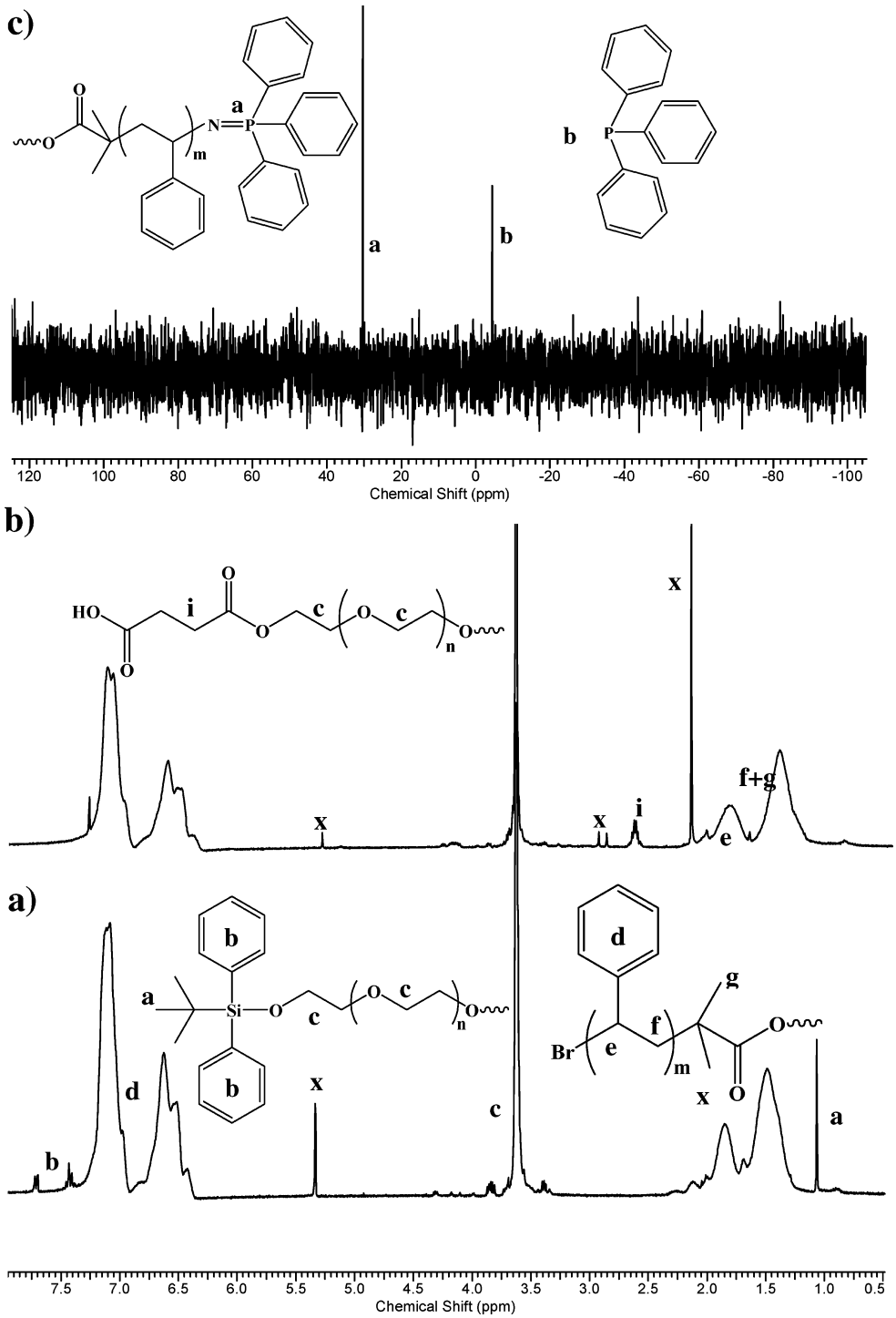

Figure 2. (a) $(Br)_2$-**S**-$(TBDPS)_2$, (b) ^1H NMR spectrum of $(Br)_2$-**S**-$(COOH)_2$, and (c) ^{31}P NMR of $((Ph)_3P{=}N)_2$-**S**-$(OH)_2$ and $P(Ph)_3$; "x" are solvent peaks.

3.6 (s, 4H, $(CH_2CH_2{-}O)n$, PEO block), 1.32 ppm (s, 6H), 1.05 (s, 18H, $C(CH_3)_3$), 2.5−2.7 (t, succinic acid). "x" are solvent signals.

The bromine functional groups of polymers **1**−**3** were each converted into amine groups in three steps to give polymers **4**−**6**, respectively, according to the procedure described in the literature.[52] The transformation of the bromine group into azide (N_3) and further to triphenylphosphine group was confirmed by the presence of a peak at about 33 ppm in the ^{31}P NMR spectrum (Figure 2c). The signal for nonchemically bonded triphenylphosphine occurs at about −10 ppm. The absence of a peak at 33 ppm following hydrolysis of triphenylphophine group yields amine functional groups. ^{31}P NMR of $(NH_2)_2$-**S**-$(OH)_2$ (δ, ppm, $CDCl_3$): −4.4 (s, triphenyl phosphine) and 30.5 (s, chemically bonded triphenylphosphine). Purification of the polymers at every stage was done by precipitation in methanol that resulted in an average yield of 65−75%.

Substrate Preparation. High-quality and freshly prepared silicon oxide surfaces of [100] silicon wafers (Semiconductor Processing Co.) were obtained through chemical etching according to the procedure adapted in our lab.[53] These wafers were chemically treated to remove any organic and inorganic contaminants from the surface according to the standard procedure: first, the wafers cut into rectangular pieces (1.5 × 1.5 cm^2) were submerged in Nanopure water (σ > 18.0 MΩ cm^{-1}) and sonicated for 10 min at a room temperature. Next, they were treated with "piranha solution" (30% concentrated hydrogen peroxide, 70% concentrated sulfuric acid, *hazardous solution!*) for 2 h to remove organic contaminants and to strip

the original silicon oxide surface layer. Finally, the substrates were abundantly rinsed with Nanopure water and dried with nitrogen stream. This treatment resulted in a fresh silicon oxide layer with a consistent thickness of about 1.2 nm with a high concentration of silanol groups. Wafer preparation was conducted in a clean room, class 100, to avoid any air contaminations on active surfaces. The surface microroughness did not exceed 0.1 nm within the 1 × 1 μm^2 surface area.

Sample Characterization. The surface behavior at the air−water interface and Langmuir−Blodgett (LB) monolayer depositions onto the silicon substrate were conducted at room temperature using an R&K 1 LB trough according to the usual procedure.[54] The 60−120 μL of dilute polymer solution (concentration less than 1 mg/L) in chloroform (HPLC grade) was deposited dropwise (5−6 drops, uniformly distributed) onto the Nanopure water surface and left to evaporate and spread evenly over a period of 30 min at room temperature. During LB deposition, the surface pressure was held constant as the submerged silicon substrate was slowly lifted up at a velocity of 3 mm/min. The LB monolayers were deposited onto the silicon substrates at two different surface pressures: low, 5 mN/m, and high, 35 mN/m (on the verge of collapsed), at a naturally occurring pH of 5.5. Additionally, polymers **3** and **6** were deposited at subphase pH of 3.2 and 8.8 at the surface pressure of 5 and 35 mN/m. The desired pH level was obtained by dropwise addition of NaOH (0.03 M) and HCl (1.3 M) and monitored using an Orion pH-meter, model 410A.

The effective thickness of the monolayers was measured with COMPEL automatic ellipsometer (InOmTech, Inc.) with an incident angle of 70° and a wavelength of 634 nm according to the well-known procedure.[55] The average thickness of the silicon oxide layer was measured prior to the monolayer deposition and later used during the ellipsometry measurement with a double-layer model was employed to calculate the monolayer thickness. The refractive index for amphiphilic copolymers was calculated by taking into account the chemical composition with the refractive index for the different blocks taken as 1.59 for PS and 1.53 for PEO.[56] The results were averaged over five independent measurements at different locations on the substrate. The standard deviations of the thicknesses measured with ellipsometry were 0.1 nm.

The LB monolayers deposited on the silicon substrates were studied with a Dimension-3000 microscope (Digital Instruments, Inc.) in the "light" tapping mode in accordance to the usual procedure adapted in our lab.[57,58] An amplitude ratio of 0.90 and higher was employed to avoid monolayer damage.[59] AFM characterizations of the deposited LB monolayers were done after drying samples in a desiccator for 24 h. The AFM scans were conducted at 1 Hz for surface areas ranging from 20 × 20 μm^2 to 1 × 1 μm^2 and for several randomly selected locations with at least 40 different images collected for each specimen. The tip radius was measured independently using gold nanoparticles as a standard reference, and only the sharpest tips were selected for scanning.[60] The AFM tip radii were between 20 and 35 nm, and the spring constants of these cantilevers were in the range 40−60 N/m. The domain heights were obtained from cross-sectional analysis, and the PS domain surface area coverage was calculated from height histograms using the bearing analysis.[61]

Results and Discussion

Air−Water Interfacial Behavior. All six copolymers demonstrated similar pressure−area behavior typical for amphiphilic compounds (Figure 3a,b). Their isotherms showed initially an almost horizontal region followed by an abrupt pressure increase at a certain surface area before reaching the collapsed region at a smaller surface area.[62] Polymers **1** and **4** showed a prominent appearance of a pseudoplateau. In general, the appearance of a significant pseudoplateau is associated with circular domain surface microstructure.[39] The surface areas per molecule, A_0, derived from the isotherms are summarized in Table 3. As clear from these

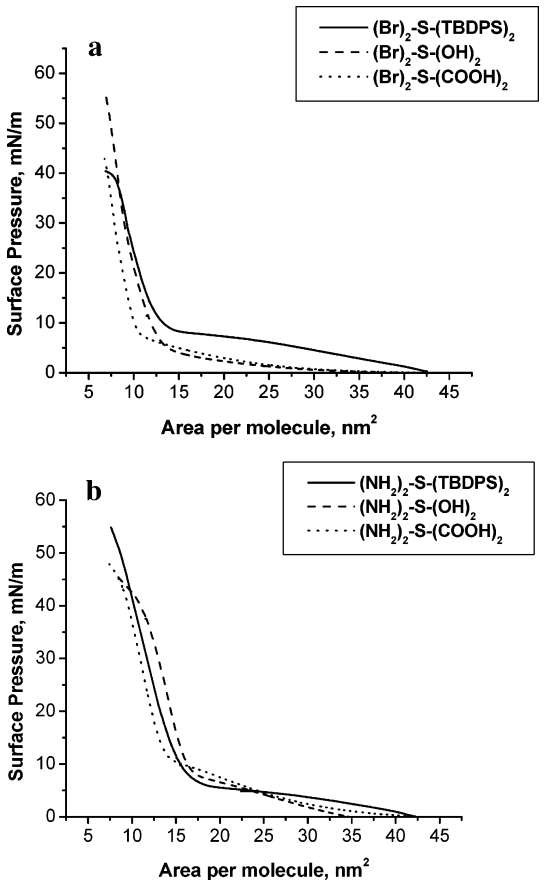

Figure 3. Langmuir isotherms of (a) (Br)$_2$-S-(Y)$_2$ and (b) (NH$_2$)$_2$-S-(Y)$_2$. Y is TBDPS, OH, or COOH.

Table 3. Surface Area per Molecule and PEO Thickness As Determined from Langmuir Isotherms

no.	polymer	A_0, nm^2	h_{PEO}, nm
1	(Br)$_2$-**S**-(TBDPS)$_2$	13.1	1.6
2	(Br)$_2$-**S**-(OH)$_2$	11.3	1.8
3	(Br)$_2$-**S**-(COOH)$_2$	10.4	2.0
4	(NH$_2$)$_2$-**S**-(TBDPS)$_2$	16.9	1.2
5	(NH$_2$) $_2$-**S**-(OH)$_2$	15.3	1.4
6	(NH$_2$)$_2$-**S**-(COOH)$_2$	14.2	1.5

data, star copolymers with Br-terminated PS arms (polymers **1**−**3**) exhibited smaller surface area per molecule (by 25−30%) or more compact packing in the condensed state as compared to star copolymers with NH$_2$-terminated PS arms (polymers **4**−**6**). This difference indicates that fully hydrophobic PS arms can be easier displaced from the air−water interface into hydrophobic domains by lateral compression while the presence of the amine terminal groups keeps hydrophobic PS arms more spread.

Changing the nature of the terminal groups of the hydrophilic PEO arms from hydrophobic (TBDPS) to hydrophilic (OH and COOH) decreased the surface area per molecule in the condensed state by 25% irrespective of the terminal groups of the PS arms (Table 3). This is a clear sign of easier desorption of PEO arms with hydrophilic terminal groups into the water subphase which results in more compact overall packing of molecules. In all cases, star copolymers with the bulky TBDPS terminal hydrophobic groups occupy the largest surface areas. The most compact packing of the star molecules at the air−water interface is achieved when compact hydrophobic Br groups at the ends of PS arms are combined with hydrophilic and polar carboxylic

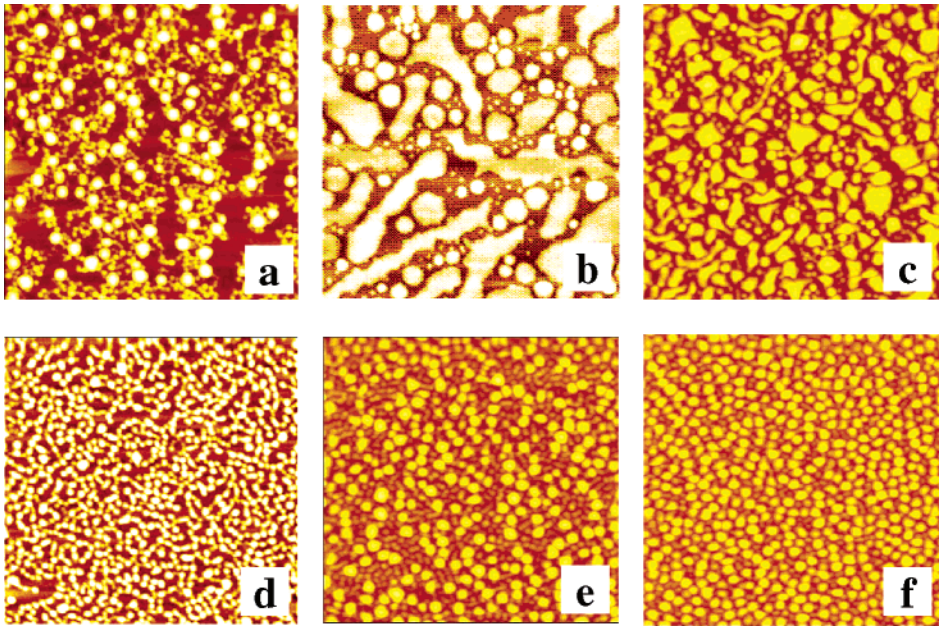

Figure 4. AFM topography of (a) $(Br)_2$-S-$(TBDPS)_2$, (b) $(Br)_2$-S-$(OH)_2$, (c) $(Br)_2$-S-$(COOH)_2$, (d) $(NH_2)_2$-S-$(TBDPS)_2$, (e) $(NH_2)_2$-S-$(OH)_2$, and (f) $(NH_2)_2$-S-$(COOH)_2$. Monolayers were deposited at surface pressure, $p = 5$ mN/m. Scan area is 2×2 μm^2. Height is 10 nm.

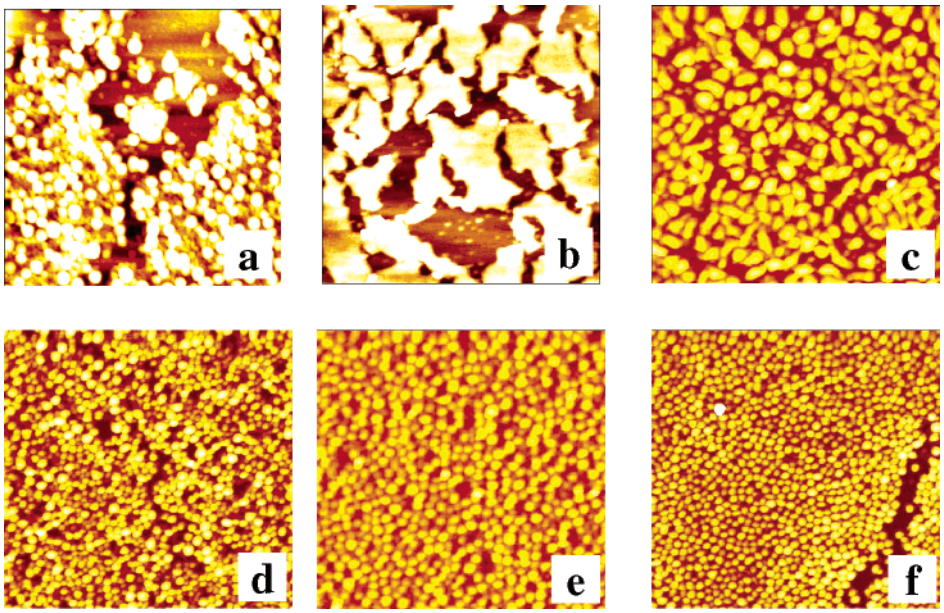

Figure 5. AFM topography of (a) $(Br)_2$-S-$(TBDPS)_2$, (b) $(Br)_2$-S-$(OH)_2$, (c) $(Br)_2$-S-$(COOH)_2$, (d) $(NH_2)_2$-S-$(TBDPS)_2$, (e) $(NH_2)_2$-S-$(OH)_2$, and (f) $(NH_2)_2$-S-$(COOH)_2$. Monolayer were deposited at surface pressure, $p = 35$ mN/m. Scan area is 2×2 μm^2. Height is 10 nm.

terminal groups for PEO arms, thus making the tendencies of different arms to escape from the interface into water subphase (PEO-COOH) and air (PS-Br) stronger (Table 3).

Surface Morphology. Surface morphology of amphiphilic star copolymers differs for different combinations of the terminal groups despite that their overall chemical composition remains very similar: PEO chains of molecular weight of 7500 each are combined with PS chains of 14 000 each, resulting in a volume fraction PEO of 32%, which is favorable for cylindrical morphology (Table 1).[23] For amphiphilic copolymers of the type A_nB_m with a particular composition, the bulk morphology can be predicted using a Milner's phase diagram, which takes into account an asymmetry of the molecular architecture.[63] This diagram predicts cylindrical morphology for star copolymers studied here as was discussed in detailed earlier.[23]

Larger area scans (10×10 μm^2 and higher) show the uniformity of all of the LB monolayers (not shown). Figures 4 and 5 show higher-resolution AFM images of LB monolayers transferred onto the silicon substrate at different surface pressures. As expected from the isotherm shape, circular domains were indeed observed for some polymers. This is indicative of the hydrophilic PEO chains being surface-anchored, a well-understood phenomenon caused by the presence of bulky hydrophobic terminal groups (TBDPS).[39] A replacement of functional groups resulted in changing surface morphology (Figure 4). The circular domains of polymer **1** are

Table 4. Monolayer Thickness and Domain Heights at Various Surface Pressures at pH = 5.5[a]

		monolayer thickness, nm				domain heights, nm	
		ellipsometry		calculated			
no.	polymer	P1	P2	P1	P2	P1	P2
1	$(Br)_2$-**S**-$(TBDPS)_2$	2.3	3.9	2.8	3.6	4.3	6.0
2	$(Br)_2$-**S**-$(OH)_2$	3.8	4.1	4.1	4.0	6.9	6.6
3	$(Br)_2$-**S**-$(COOH)_2$	3.4	4.5	4.1	4.4	5.4	5.4
4	$(NH_2)_2$-**S**-$(TBDPS)_2$	2.5	3.9	2.8	3.4	4.2	4.5
5	$(NH_2)_2$-**S**-$(OH)_2$	2.9	4.2	3.4	3.2	6.0	4.5
6	$(NH_2)_2$-**S**-$(COOH)_2$	2.7	3.7	3.4	3.5	5.0	4.5

[a] Surface pressure P1 is 5 mN/m and P2 is 35 mN/m.

not as uniform as those seen for polymer **4**. Overall, the domain morphology is much finer and uniform for all star copolymers with NH_2-terminated PS arms.

Mixed small-medium circular and circular-cylindrical domain morphology was observed for all star copolymers with Br-terminated PS arms (Figures 4 and 5). Lateral domain sizes were widely distributed from 10 to 100 nm. Effective monolayer thickness measured using ellipsometry was within 2.3−3.8 nm for all monolayers studied at low pressure and increased to 3.7−4.5 nm for higher compressions (Table 4). These values closely resemble those measured by AFM affirming the accuracy of the predicted micelle conformation on solid substrates.[22] The domain heights were much more uniform and stayed within 4.3−6.9 nm for all surface pressures applied here (Table 4). The domain heights increased slightly with pressure for both star copolymers with hydrophobic terminal groups of PEO chains but remained unchanged for star copolymers with OH- and COOH-terminated PEO chains (Table 4). The surface coverage with domains was within 28−48% as estimated from the AFM images taking into account the tip convolution.

The replacement of the PEO hydrophobic end groups with hydrophilic OH groups resulted in decreased stability of the circular microstructure and the appearance of mixed circular and cylindrical domains with a wide distribution of lateral sizes within 10−200 nm. On the other hand, the replacement of the Br terminal groups with NH_2 groups shifted the morphological pattern to fine circular domains with an average diameter below 50 nm. This indicates that the hydrophobic−hydrophilic combination enhances the phase separation leading to stable circular domain morphology. Moreover, phase separation driven by the contrasting nature of polymer chains and end-functional groups is more effective in controlling aggregation of the hydrophobic PS chains as compared to the hydrophilic PEO chains. However, it is worthwhile to note that the stability of a fine circular domain can be easily disturbed by, e.g., the capillary forces acting along the edges of the substrates as visible from well-developed lamellar and cylindrical morphologies in these surface areas (Figure 6).

High-resolution imaging of the domain morphology of star copolymers studied here showed very uniform heights of circular and cylindrical domains (within 2−4 nm above the surrounding media) and diameters below 50 nm (Table 4, Figure 7). Considering that the supporting substrate is hydrophilic, the general schematics of the surface distribution of individual PS domains and a surface layer composed mainly of PEO chains can be presented as that in Figure 7, in agreement with the known models for linear PS−PEO block copolymers layers on solid surfaces.[22,43,64] This general model will

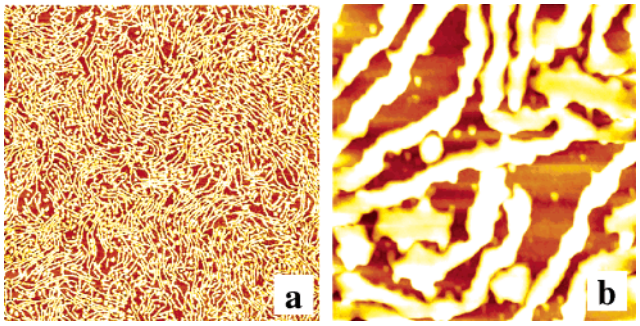

Figure 6. AFM topography of $(Br)_2$-S-$(OH)_2$ obtained at the edge of the substrate. Scan area is 20 × 20 μm^2 for (a) and 2 × 2 μm^2 for (b). Height is 30 nm.

be elaborated below into a specific model for star copolymers with different functionalized terminal groups considering current results.

Effect of Subphase pH. As described by Le Châtelier's principle,[65] ionizable groups undergo reversible protonation−deprotonation transition, which can significantly affect interfacial behavior of the functionalized star copolymers. The two polymer samples studied under varying pH are $(Br)_2$-**S**-$(COOH)_2$ and $(NH_2)_2$-**S**-$(COOH)_2$. The pK_a values of carboxylic and amine functional groups at room temperature is estimated to be about 5.6 (succinic acid) and between 4.6 (aniline) and 10.6 (benzylamine), respectively.[66] Thus, Langmuir isotherms were collected in the range of pH from 3.2 to 10.6 (Figure 8). However, compression at pH = 10.6 revealed a monotonic nonequilibrium isotherm, indicating hydrolysis of the ester linkages. The pH values within pH = 3.2−8.8 covered the pK_a values for both star copolymers. Langmuir isotherms of polymer **3**, $(Br)_2$-**S**-$(COOH)_2$, and polymer **6**, $(NH_2)_2$-**S**-$COOH)_2$, at pH of 3.2, 5.5, and 8.8 are shown in parts a and b of Figure 8, respectively. The shape of the Langmuir isotherms is consistent for all pHs with overall stability of the monolayers (pressure for a precollapsed state) decreasing significantly for higher pH (Figure 8). Highest stability (higher collapsed pressure) for both star copolymers was observed for the lowest pH studied here. The surface areas per molecule of the samples showed a slight decrease (within 10%) with increasing pH (Table 5).

The surface morphology underwent notable transformation for both star copolymers with changing pH level of the subphase (Figure 9). The irregular mixed morphology at low pH was replaced with a much finer circular morphology in Br-terminated star copolymer and an ideal uniform circular morphology for NH_2-terminated star copolymer for all surface pressures. The monolayer thicknesses and domain heights did not change significantly at various pHs (Table 6). These results clearly demonstrate that the ionization of the terminal groups can shift equilibrium and change the domain morphology as follows: first, higher ionization of the carboxylic groups results in higher solubility of PEO chains, causing easier submergence in the water subphase. Second, desorption of PEO chains from the air−water interface into the subphase causes the reduction of the surface area occupied by a molecule, reduces lateral compression resistance, and shifts a balance toward circular morphology because of the reduced content of the minor component (PEO) at the surface as predicted by Milner's diagram.[67] Replacement of Br terminal groups of PS arms to amine does change the

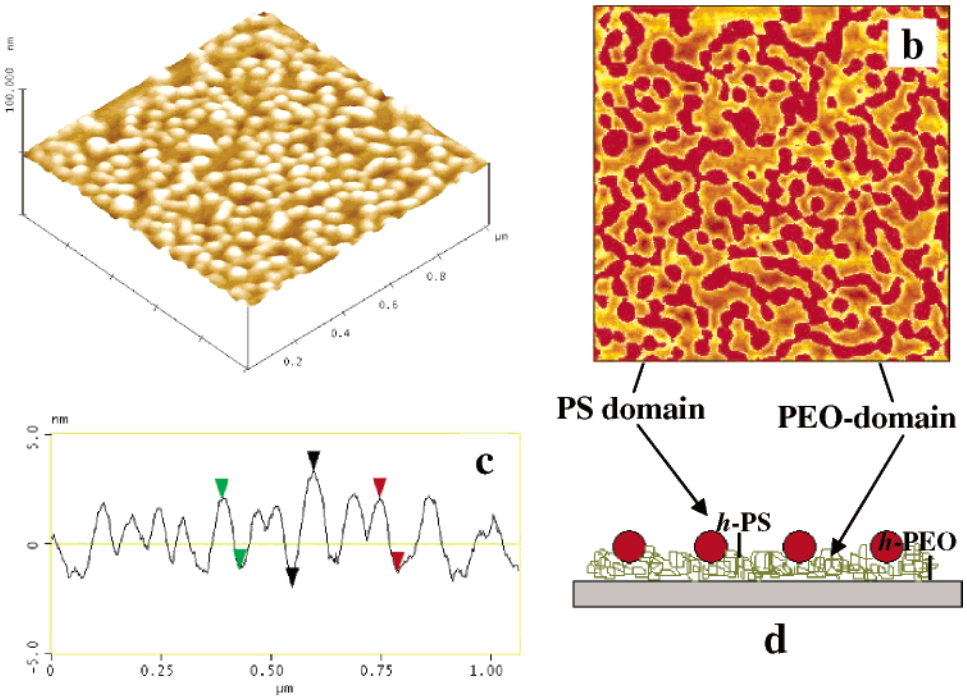

Figure 7. A representative three-dimensional surface plot (a) with its corresponding profile (b) and cross-sectional analysis with scan size 1 × 1 μm (c) for $(NH_2)_2$-**S**-$(TBDPS)_2$ star copolymer deposited at $p = 5$ mN/m; cartoon representation of deposited PEO–PS copolymer on the silicon wafer substrate: ***h***-PS is height of PS domain, and ***h***-PEO is height of PEO domain (d).

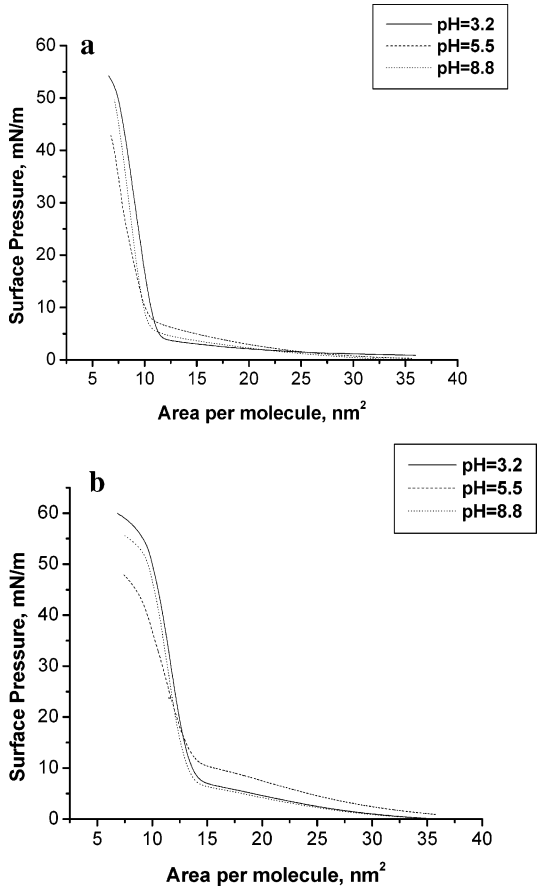

Figure 8. Langmuir isotherms of (a) $(Br)_2$-S-$(COOH)_2$ and (b) $(NH_2)_2$-S-$(COOH)_2$ at various pH levels.

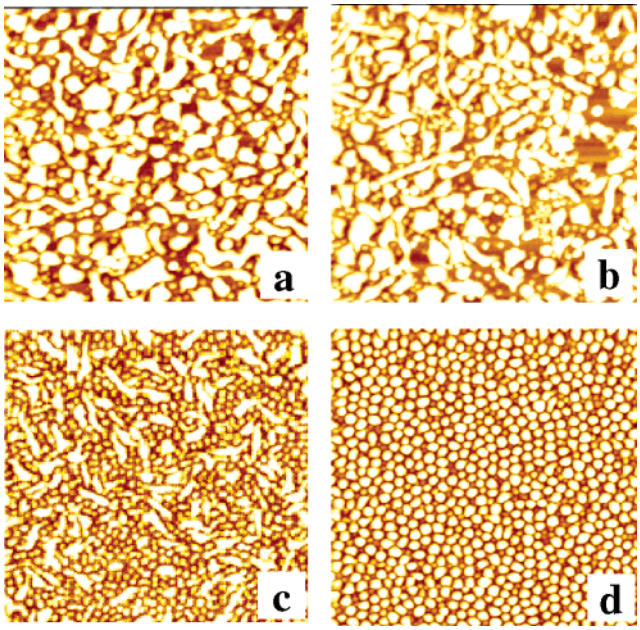

Figure 9. AFM topography of $(Br)_2$-S-$(COOH)_2$ (a and b) and $(NH_2)_2$-S-$(COOH)_2$ (c and d) at pH = 3.2 (a and c) and pH = 8.8 (b and d). Monolayers were deposited at surface pressure $p = 5$ mN/m. Scan areas are 2 × 2 μm^2. Height is 10 nm.

Table 5. Surface Area per Molecule of $(Br)_2$-S-$(COOH)_2$ and $(NH)_2$-S-$(COOH)_2$ at Various pHs

	A_0, nm^2		
polymer	pH = 3.2	pH = 5.5	pH = 8.8
$(Br)_2$-**S**-$(COOH)_2$	11.2	10.4	10.4
$(NH_2)_2$-**S**-$(COOH)_2$	14.0	14.2	13.7

overall pattern because the ionization of amine group is modest within the pH range tested.

Micellization at the Air–Water Interface. Here, we discuss how the microphase separation of dissimilar polymer chains at the air–water interface influenced by the nature of their terminal groups governs their surface morphology and microstructure. Generally, amphiphilic star copolymer residing at the air–water interface adopts molecular conformation with PEO

Table 6. Monolayers Thicknesses and Domain Heights at pH = 3.2 and 8.8

	ellipsometry, nm		domain height, nm	
polymer	P = 5 mN/m	P = 35 mN/m	P = 5 mN/m	P = 35 mN/m
$(Br)_2$-**S**-$(COOH)_2$ (pH = 3.2)	2.4	3.7	5.9	7.5
$(Br)_2$-**S**-$(COOH)_2$ (pH = 8.8)	2.6	3.5	6.5	8.3
$(NH_2)_2$-**S**-$(COOH)_2$ (pH = 3.2)	2.1	3.3	5.2	5.6
$(NH_2)_2$-**S**-$(COOH)_2$ (pH = 8.8)	2.3	3.5	4.8	5.6

chains in a close contact with the water subphase and PS chains forming individual domains above the air−water interface. Two possible cases are illustrated in Figure 10: case 1, in which the hydrophilic PEO chains with modest water solubility are spread on the water surface in randomly coiled conformation beneath PS domains, and case 2, where the PEO chains are submerged into the water subphase. An occurrence of one of the two possible scenarios is defined by overall chemical composition, the length of PEO chains, the presence of specific terminal groups, and the surface pressure. For example, as demonstrated by Zhu et al., hydrophobic terminal groups attached to hydrophilic PEO chains anchor them at the water surface, preventing neighboring micelles from merging. Hydrophilic end-functional groups, on the other hand, allow the hydrophilic PEO chains to "sink" into the water subphase, under even very low surface pressure.[39]

Considering that the model presented in Figure 10a can be applied to star copolymers with hydrophobic terminal groups, the molecular arrangement at high surface pressures is presented in Figure 10b. At low surface pressure, the PEO chains are mainly located at the water surface, thus preventing the aggregation of PS domains into large surface areas. Forced submergence of PEO chains at high surface pressure does not change the PS domain morphology but results in dense packing (Figure 10b). On the other hand, the presence of the hydrophilic terminal groups in PEO chains causes them to submerge into the water subphase even at low surface pressure, followed by the aggregation of PS domains at higher surface pressure (Figure 10c).

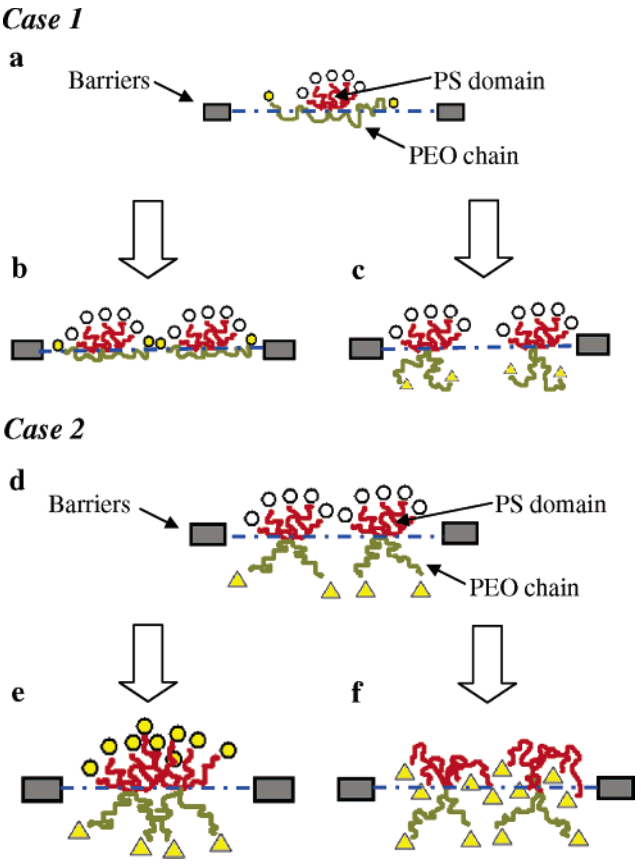

Figure 10. Amphiphilic copolymer micelles containing different terminal-functional groups at low (left) and high (right) pressures; (a, d) uncompressed states. ○ and ● are hydrophobic end groups, and ▲ marks hydrophilic end groups. Case 1: end-functional groups at hydrophilic chains. Case 2: end-functional groups at hydrophobic chains.

Adding hydrophilic amine terminal groups to the PS chains changes the aggregation behavior and prevents the lateral aggregation of PS domains. This along with the reduction of the PEO content at the water interface due to PEO desorption promotes the formation of fine circular domain morphology (Figure 10f). This phenomenon is more pronounced in star block copolymer with highly polar carboxylic terminal groups of PEO chains. Generally, the alteration of the functional groups attached to the hydrophobic PS chains plays a more important role in the controlling lateral segregation and the formation of stable circular domain morphology. In addition, ionization of the carboxylic terminal groups at higher pH results in a higher level of PEO chains sinking in the water subphase, which further promotes the formation of nanoscale circular morphology.

Conclusions

In conclusion, a series of end-functionalized heteroarm PEO−PS star copolymers were synthesized, and their surface behavior was studied. We observed that the opposite nature of polymer chains and its end groups (hydrophobic chains−hydrophilic ends or hydrophilic chains−hydrophobic ends) is substantial in the formation of stable circular morphology, rather than cylindrical morphology expected for the given chemical composition of star block copolymers. The variation of end groups of hydrophobic chains was found to be more effective in creating stable and very fine, nanoscale circular domain morphology. For carboxyl- and amine-terminated star polymer, $(COOH\text{-}PEO)_2$-$(PS\text{-}NH_2)_2$, the subphase pH played an important role in the formation of surface morphology due to the variable ionization of end groups.

Acknowledgment. Funding from Imperial Chemical Industries, SRF 2112 Contract, and the National Science Foundation, DMR-0308982 grant, is gratefully acknowledged.

References and Notes

(1) Voulgaris, D.; Tsitsilianis, C.; Esselink, F. J.; Hadziioannou, G. *Polymer* **1998**, *39*, 6429.
(2) Narrainen, A. P.; Pascual, S.; Haddleton, D. M. *J. Polym. Sci., Part A: Polym. Chem.* **2002**, *40*, 439.
(3) Voulgaris, D.; Tsitsilianis, C. *Macromol. Chem. Phys.* **2001**, *202*, 3284.
(4) Ornatska, M.; Bergman, K. N.; Rybak, B.; Peleshanko, S.; Tsukruk, V. V. *Angew. Chem.* **2004**, *43*, 5246.
(5) Ornatska, M.; Peleshanko, S.; Genson, K. L.; Rybak, B.; Bergman, K. N.; Tsukruk, V. V. *J. Am. Chem. Soc.* **2004**, *126*, 9675.
(6) Ornatska, M.; Peleshanko, S.; Rybak, B.; Holzmueller, J.; Tsukruk, V. V. *Adv. Mater.* **2004**, *16*, 2206.
(7) Boyce, J. R.; Shirvanyants, D.; Sheiko, S. S.; Ivanov, D. A.; Qin, S.; Boerner, H.; Matyjaszewski, K. *Langmuir* **2004**, *20*, 6005.
(8) Lord, S. J.; Sheiko, S. S.; LaRue, I.; Lee, H.; Matyjaszewski, K. *Macromolecules* **2004**, *37*, 4235.

(9) Kanaoka, S.; Kanaoka, S.; Nakata, S.; Yamaoka, H. *Macromolecules* **1992**, *25*, 6414.
(10) Kanaoka, S.; Sawamoto, M.; Higashimura, T. *Macromolecules* **1993**, *26*, 254.
(11) Genson, K. L.; Hoffman, J.; Teng, J.; Zubarev, E. R.; Vaknin, D.; Tsukruk, V. V. *Langmuir* **2004**, *20*, 9044.
(12) Luzinov, I.; Minko, S.; Tsukruk, V. V. *Prog. Polym. Sci.* **2004**, *29*, 635.
(13) Holzmueller, J.; Genson, K. L.; Park, Y.; Yoo, Y.-S.; Park, M.-H.; Lee, M.; Tsukruk, V. V. *Langmuir* **2005**, *21*, 6392.
(14) Kanaoka, S.; Nakata, S.; Yamaoka, H. *Macromolecules* **2002**, *35*, 4564.
(15) Herman, D. S.; Kinning, D. J.; Thomas, E. L.; Fetters, L. J. *Macromolecules* **1987**, *20*, 2940.
(16) Tselikas, Y.; Hadjichristidis, N.; Lescanec, R. L.; Honeker, C. C.; Wohlgemuth, M.; Thomas, E. L. *Macromolecules* **1996**, *29*, 2290.
(17) Pochan, D. J.; Gido, S. P.; Pispas, S.; Mays, J. W.; Ryan, A. J.; Fairclough, P. A.; Hamley, I. W.; Terrill, N. J. *Macromolecules* **1996**, *29*, 5091.
(18) Lin, Y.-H.; Teng, J.; Zubarev, E. R.; Shulha, H.; Tsukruk, V. V. *Nano Lett.* **2005**, *5*, 491.
(19) Julthongpiput, D.; Lin, Y.-H.; Teng, J.; Zubarev, E. R.; Tsukruk, V. V. *J. Am. Chem. Soc.* **2003**, *125*, 15912.
(20) Pochan, D. J.; Gido, S. P.; Pispas, S.; Mays, J. W. *Macromolecules* **1996**, *29*, 5099.
(21) Francis, R.; Taton, D.; Logan, J. L.; Masse, P.; Gnanou, Y.; Duran, R. S. *Macromolecules* **2003**, *36*, 8253.
(22) Francis, R.; Skolnik, A. M.; Carino, S. R.; Logan, J. L.; Underhill, R. S.; Angot, S.; Taton, D.; Gnanou, Y.; Duran, R. S. *Macromolecules* **2002**, *35*, 6483.
(23) Peleshanko, S.; Jeong, J.; Gunawidjaja, R.; Tsukruk, V. V. *Macromolecules* **2004**, *37*, 6511.
(24) Peleshanko, S.; Gunawidjaja, R.; Jeong, J.; Shevchenko, V. V.; Tsukruk, V. V. *Langmuir* **2004**, *20*, 9423.
(25) Gido, S. P.; Lee, C.; Pochan, D. J.; Pispas, S.; Mays, J. W.; Hadjichristidis, N. *Macromolecules* **1996**, *29*, 7022.
(26) Hadjichristidis, N.; Pitsikalis, M.; Iatrou, H.; Pispas, S. *Macromol. Rapid Commun.* **2003**, *24*, 979.
(27) Pispas, S.; Avgeropoulos, A.; Hadjichristidis, N.; Roovers, J. *J. Polym. Sci., Part B: Polym. Phys.* **1999**, *37*, 1329.
(28) Houli, S.; Iatrou, H.; Hadjichristidis, N.; Vlassopoulous, D. *Macromolecules* **2002**, *35*, 6592.
(29) Okamoto, S.; Hasegawa, H.; Hashimoto, T.; Fujimoto, T.; Zhang, H.; Kazama, T.; Takano, A.; Isono, Y. *Polymer* **1997**, *38*, 5275.
(30) Zhao, Y.; Shuai, X.; Chen, C.; Xi, F. *Chem. Commun.* **2004**, 1608.
(31) Webster, O. W. *Science*, **1991**, *251*, 887.
(32) Pispas, S.; Hadjichristidis, N. *J. Polym. Sci., Part A: Polym. Chem.* **2000**, *38*, 3791.
(33) Patil, O. A.; Schulz, D. N.; Novak, B. M. *Functional Polymers: Modern Synthetic Methods and Novel Structures; ACS Symp. Ser.* **1998**, *704*, 1.
(34) Barentin, C.; Joanny, J. F. *Langmuir* **1999**, *15*, 1802.
(35) Hammouda, B.; Ho, D. L.; Kline, S. *Macromolecules* **2004**, *37*, 6932.
(36) Pispas, S.; Hadjichristidis, N. *J. Polym. Sci., Part A: Polym. Chem.* **2000**, *38*, 3791.
(37) Dormidontova, E. E. *Macromolecules* **2004**, *37*, 7747.
(38) Devereaux, C. A.; Baker, S. M. *Macromolecules* **2002**, *35*, 1921.
(39) Zhu, J.; Eisenberg, A.; Lennox, R. B. *Macromolecules* **1992**, *25*, 6547.
(40) Baker, S. M.; Leach, K. A.; Devereaux, C. E.; Gragson, D. E. *Macromolecules* **2000**, *33*, 5432.
(41) Seo, Y.; Paeng, K.; Park, S. *Macromolecules* **2001**, *34*, 8735.
(42) Zhu, J.; Lennox, B.; Eisenberg, A. *J. Phys. Chem.* **1992**, *96*, 4727.
(43) Cox, J. K.; Yu, K.; Eisenberg, A.; Lennox, R. B. *Phys. Chem. Chem. Phys.* **1999**, *1*, 4417.
(44) Knoll, A.; Horvat, A.; Lyakhova, K. S.; Grausch, G.; Sevink, G. J. A.; Zvelindovsky, A. V.; Magerle, R. *Phys. Rev. Lett.* **2002**, *89*, 035501.
(45) Zhu, J.; Eisenberg, A.; Lennox, R. B. *Macromolecules* **1992**, *25*, 6566.
(46) Fauré, M. C.; Bassereau, P.; Lee, L. T.; Manelle, A.; Lheveder, C. *Macromolecules* **1999**, *32*, 8538.
(47) Peleshanko, S.; Jeong, J.; Shevchenko, V.; V.; Petrash, S.; Tsukruk, V. V. *Macromolecules* **2004**, *37*, 7497.
(48) Huang, H.-M.; Liu, I.-C.; Tsiang, C.-C. R. *Polymer* **2004**, *46*, 955.
(49) Greene, T. W.; Wuts, P. G. M. *Protective Groups in Organic Synthesis*, 3rd ed.; Wiley-Interscience: New York, 1999.
(50) Carnahan, M. A.; Grinstaff, M. W. *Macromolecules* **2001**, *34*, 7648.
(51) Luman, N. R.; Smeds, K. A.; Grinstaff, M. W *Chem.—Eur. J.* **2003**, *9*, 5618.
(52) Coessens, V.; Nakagawa, Y.; Matyjaszewski, K. *Polym. Bull. (Berlin)* **1998**, *40*, 135.
(53) Tsukruk, V. V.; Bliznyuk, V. N. *Langmuir* **1998**, *14*, 446.
(54) Ulman, A. *An Introduction to Ultrathin Organic Films: From Langmuir–Blodgett to Self-Assembly*; Academic Press: Boston, MA, 1991.
(55) Azzam, R. M. A.; Bashara, N. M. *Ellipsometry and Polarized Light*; North-Holland Pub. Co.: New York, 1977.
(56) Immergut, E. H.; Grulke, E. A. *Polymer Handbook*; John Wiley & Sons: New York, 1999.
(57) Tsukruk, V. V. *Rubber Chem. Technol.* **1997**, *70*, 430.
(58) Tsukruk, V. V.; Reneker, D. H. *Polymer* **1995**, *36*, 1791.
(59) Magonov, S. N.; Elings, V.; Whangbo, M.-H. *Surf. Sci.* **1997**, *375*, L385.
(60) Guzonas, D.; Boils, D.; Hair, M. L. *Macromolecules* **1991**, *24*, 3383.
(61) Magonov, S. N. *Surface Analysis with STM and AFM: Experimental and Theoretical Aspects of Image Analysis*; VCH: Weinheim, Germany, 1996.
(62) Roberts, G. *Langmuir–Blodgett Films*; Plenum Press: New York, 1990.
(63) Grayer, V.; Dormidontova, E. E.; Hadziioannou, G.; Tsisilianis, C. *Macromolecules* **2000**, *33*, 6330.
(64) Gonçalves da Silva, A. M.; Filipe, E. J. M.; d'Oliveira, J. M. R.; Martinho, J. M. G. *Langmuir* **1996**, *12*, 6547.
(65) Whitten, K. W.; Davis, R. E.; Peck, L. M.; Stanley, G. G. *General Chemistry*, 7th ed.; Brooks Cole, 2003.
(66) Lide, D. R. *CRC Handbook of Chemistry and Physics*, 76th ed.; CRC Press: Boca Raton, FL, 1996.
(67) Milner, S. T. *Macromolecules* **1994**, *27*, 2333.

MA050463V